Acta Geochim (2021) 40(2):212–224
https://doi.org/10.1007/s11631-021-00450-w

ORIGINAL ARTICLE

Effects of geosorbent and solution properties on sorption and desorption of PAHs

Hui Dong[1,2] · Baohua Xiao[1]

Received: 5 October 2020 / Revised: 15 December 2020 / Accepted: 4 January 2021 / Published online: 15 January 2021
© Science Press and Institute of Geochemistry, CAS and Springer-Verlag GmbH Germany, part of Springer Nature 2021

Abstract Characteristics of phenanthrene and pyrene's sorption and desorption on two local soils in solutions of simulated groundwater, simulated lung fluid, and simulated saliva were studied with batch equilibrium experiments to understand the fate of PAHs in the karst region of southwestern China and to assess the environmental exposure and the health risk of PAHs. The results showed that the sorption and desorption isotherms of phenanthrene and pyrene on two target soils in the three solution systems could be adequately described by the Freundlich model, while the fitted isotherm parameters for the simulated groundwater solution distinguished notably from those for the simulated body fluid solutions. For the sorption experiments, in the simulated groundwater, the n values were 0.722 and 0.672 for phenanthrene and were 0.724 and 0.663 for pyrene, respectively, on the yellow soil and the limestone soil; The $log\ K_F$ values were 3.118 and 3.323 for phenanthrene and were 3.648 and 3.846 for pyrene, respectively, on the yellow soil and the limestone soil. In the simulated body fluids, the n values for phenanthrene and pyrene ranged from 0.622 to 0.836 and from 0.590 to 0.865, respectively, and the $log\ K_F$ values of phenanthrene and pyrene ranged from 2.845 to 3.327 and from 3.344 to 3.779, respectively. For the desorption experiments, in the simulated groundwater, the n values were 0.662 and 0.744 for phenanthrene and were 0.702 and 0.647 for pyrene, respectively, on the yellow soil and the limestone soil. The $log\ K_F$ values were 3.666 and 3.686 for phenanthrene and were 4.128 and 4.225 for pyrene, respectively, on the yellow soil and the limestone soil. In the simulated body fluids, the n values for phenanthrene and pyrene ranged from 0.612 to 0.668 and from 0.631 to 0.819, respectively, and the $log\ K_F$ values of phenanthrene and pyrene ranged from 3.134 to 3.407 and from 3.533 to 3.839, respectively. The limestone soil had relatively higher $log\ K_F$ values but lower K_{OC} values compared to those of the yellow soil, indicated that the nature of sorbent soils played the dominant role in sorption and desorption behaviors of PAHs. The experimental results showed a remarkable differences in sorption and desorption behaviors of PAHs in simulated body fluids and groundwater. The nonlinearities of measured isotherms and the measured sorption capacities of soils in simulated body fluids were significantly lower than corresponding those in the simulated groundwater, and *HI* values for simulated body fluids systems were significantly smaller than corresponding those for the simulated groundwater systems. The results underscore cautions in assessing environmental exposure and health risks of PAHs based on their sorption–desorption data in simulated groundwater as this is traditionally done.

Keywords PAHs · Sorption–desorption · Simulated body fluids · Yellow soil · Limestone soil

1 Introduction

Polycyclic aromatic hydrocarbons (PAHs) as a type of anthropogenic pollution are formed mainly during incomplete combustion of fossil fuels and biomass and exist ubiquitously in the natural environment. PAHs are a class

---

✉ Baohua Xiao
xiaobaohua@mail.gyig.ac.cn

[1] State Key Laboratory of Environmental Geochemistry, Institute of Geochemistry, Chinese Academy of Sciences, Guiyang 550018, China

[2] University of Chinese Academy of Sciences, Beijing 100049, China

of chemicals containing only carbon and hydrogen with structures of multiple aromatic rings. Several PAHs are considered to induce carcinogenic, mutagenic, and teratogenic effects on humans (Barnier et al. 2014). Environmental PAHs concentrations have increased in many industrialized and developing countries in decades. The high emissions of PAHs, more than 116,000 tons/year, resulted in heavy contamination of various environmental media (Wang et al. 2011a, b; Xia et al. 2013). Due to the hydrophobicity, PAHs tend to sorb on soil and sediment particles while their aqueous concentrations are relatively low (Wilcke 2000; Ni et al. 2008; Yang et al. 2014; Yu et al. 2014). Sorption and desorption on soil particles are important processes governing the fate of PAHs in the environment. A comprehensive understanding of sorption and desorption behaviors of PAHs in soils and sediments is a prerequisite for accurately evaluating their environmental risk and human exposure.

Soil, sediment, and aquifer materials are highly heterogeneous and comprise various inorganic and organic components, in which the soil organic matter (SOM) is the primary sorptive component for PAHs. SOM consists of a wide range of organic molecules formed through various oxidation, reduction, condensation, and polymerization processes under different biological and geological environments (Huang 1997). The sorption of hydrophobic compounds from water to SOM is thermodynamically driven primarily by the hydrophobic effect which is caused by water molecules in solution forming an ordered ‘cage’ around hydrophobic portions of the organic molecule (Pignatella 1998). Previous research had proven that SOM is the dominant component for HOCs sorption, and the SOM heterogeneity has major impacts on the rates and extents of sorption. A conceptual dual-domain model has been proposed which suggested that SOM may consist of two physically and chemically different types of domains. In the hypothesis, a ‘soft’ rubbery amorphous domain contains fulvic acid and humic acid which are characterized by linear sorption and desorption, while a ‘hard’ glassy condensed domain may consist of kerogen, black carbon, and humin which are responsible for nonlinear sorption and desorption (Weber and Huang 1996; Xing et al. 1997; Xiao et al. 2004).

The physical conformation of SOM could be one of the key factors affecting the interaction between SOM and hydrophobic organic chemicals (HOCs) like PAHs. Cornelissen and Gustafsson (2005) summarized the sorption properties for a wide range of carbonaceous geosorbents. The contribution of carbonaceous geosorbents to the overall sorption of a given HOC varied over a wide range, which was led by different physicochemical properties. SOM originated from a different source has quite different structural and physicochemical properties, and this heterogeneous nature should have a strong impact on equilibria and rates of HOC’s sorption and desorption. Quality of SOM significantly influenced the sorption–desorption of HOCs by soils. The value of organic carbon normalized distribution coefficient (K_{oc}) increased with increasing aromaticity of organic phases while decreased with increasing effective polarity. For example, young, surface soil organic matter had lower sorption capacity than the old organic matter in shale (Xing 1997). The lower the H/C atomic ratio of the SOM is, the more aromatic and hydrophobic the SOM is, and the greater the driving force is for sorption. SOM with a lower H/C ratio coupled with greater cross-linkage of the matrix could exhibit stronger site-limited sorption at external and internal surfaces (Huang and Webber 1997).

Among the various types of SOMs, geological matured humic materials, kerogen, for example, have been shown to play important roles in HOC sorption (Huang 1997). Some studies showed that sorption of HOCs by SOM was controlled by aromatic carbon (Chin et al.1997; Perminova et al. 1999; Abelmann et al. 2005; Pan et al. 2007), while others indicated that the humin fraction of SOM has a significantly higher affinity with HOCs than other components (Ding et al. 2002; Gunasekara and Xing 2003; Pan et al. 2007). Humic acid aggregates could be considered as an analogy to well-structured organic polymers (LeBoeuf and Weber 1997, 2000a, b; Young and LeBoeuf 2000; Huang et al. 2003). Humin may consist of complex SOM ranging from unaltered or less-altered biopolymers such as lignin, polysaccharides, mineral-bound lipids, and humic acid-like materials (Huang et al. 2003). It is known that resistance to molecular diffusion within the pores whose sizes are slightly larger than sorbate molecules is much greater than within the pores of sizes several times larger than sorbate molecules. Sorptive reactivity exhibited different processes because of different origins and heterogeneous physicochemical properties. The rates and equilibria of sorption/desorption appear to coincide with the types of SOM and physicochemical properties. Humic and fulvic acids are amorphous with the higher O/C and H/C ratios and could be swollen by water molecules, sorption onto this domain would be fast and linear. In contrast, humin is condensed with lower O/C and H/C ratios, its sorption isotherm would be nonlinear, and the rate is relatively slow.

It is often observed that desorption isotherm is not the same as sorption isotherm, suggesting the existence of hysteresis. The hysteresis has been reported for many compounds, including PAHs, chlorinated benzenes, phenols, pesticides, and PCBs (Pignatello 1990; Kan et al. 1994), which could be a consequence of slow sorption or desorption kinetics (Wu and Gschwend 1986; Brusseau and Rao 1989; Ball and Roberts 1991). The equilibrium distribution of HOCs was believed to be a result of a partitioning process controlled by soil organic carbon (Chiou et al. 1979). For PAHs, sorption has been correlated with the degree of aromaticity in soil humic materials (Carmichael et al. 1997). Sorption and desorption of HOCs typically include an initial rapid phase followed by a slower phase to equilibrium. The degree of hysteresis was greater for higher molecular weight PAH on the same soil, and on higher organic soil. Ghosh et al. (2001) had demonstrated for Milwaukee Harbor sediment that PAHs associated with clay/silt particles desorbed faster with low desorption activation energies, while PAHs associated with coal-derived material desorbed at a much slower rate with high desorption activation energies. Several previous studies showed that a fraction of sorbed HOCs desorbed very slowly (Kan et al. 1994; Carmicheal et al. 1997; Yang et al. 2008, 2014; Luo et al. 2012), which means desorption hysteresis exists in interaction processes between HOCs and soil/sediment particles. Heterogeneous sorption with varied sorption sites has been proposed to explain the persistent release of HOCs, whereby a fraction of HOCs is assumed to sorb on sites with high sorption energy or specific sorption sites on an organic polymer (Kan et al. 1998). Prior research had shown that entrapments of sorbed molecules within SOM and inorganic matrices are possibly the major mechanisms for the apparent hysteresis observed for HOCs (Huang and Weber 1998; Huang et al. 1998; Weber et al. 1998; Farrell et al. 1999).

PAHs are important contaminants in the karst area of southwest China since the wide and longtime of uncontrolled coal burning in this area. However, only a few studies had been done for assessing the environmental exposure and health risk of PAHs in this area. Although sorption and desorption behaviors of PAHs on geosorbents like soil and sediment have been extensively explored and underlying mechanisms have been recognized in general, the high variation of sorptive behaviors of PAHs on soils related to the high heterogeneity of soil demands much more specific data to accurately assess environmental exposure and following health risks of PAHs in a specific region. This study aimed to characterize sorption and desorption properties of PAHs on two most common soils of the karst area of southwest China, and to evaluate impacts of physical and chemical differences of soils and different aqueous solutions on sorptive behaviors of PAHs and to discuss their environmental exposure and health risk in the karst area of southwest China.

2 Materials and methods

2.1 Sorbents and sorbates

Two surface soils, the yellow soil (YS) and the lime soil (LS), were selected used as the sorbents. They were selected since they are the most common soils of the study area in southwest China and can be obtained easily. The yellow soil sample was collected at the Duxi forest park in Guiyang, China, while the lime soil sample was collected at the Maolan national forest park in Libo, China. Detailed information about the soil samples was provided elsewhere (Di et al. 2018). The soils were collected from the surface (0–12 cm), air-dried, gently ground, and let to pass through a 10 mm mesh sieve. The selected physicochemical properties of soil samples are listed in Tables 1 and 2. Two typical PAHs, phenanthrene and pyrene, were chosen as the sorbates. They were chosen because they are among the most common PAH pollutants in the study area, and their sorption properties have been extensively characterized in prior studies, which may help in comparing and better understanding interactions between PAHs and local soils. Both chemicals in HPLC grade were purchased from Sigma-Aldrich, Inc.

2.2 Solutions

The simulated groundwater solution, which is the commonly deployed aqueous solution, contained 0.005 M $CaCl_2$ and 0.001 M $NaHCO_3$ to mimic its natural conditions. NaN_3 at a level of 100 mg/L was used as the inhibitor for microorganism growth. The simulated body fluids, lung fluid, and saliva were prepared as suggested in the literature (Stopford et al. 2003; Dean and Ma 2007; Colombo et al. 2008). The compounds and their contents in simulated lung fluid and saliva are presented in Table 3. The compounds of simulated lung fluid were added exactly as the order presented in Table 3 to avoid salt precipitation, and then the solution was adjusted to pH 7.2 using a HCl solution (0.1 M). Similarly, the compounds of the simulated saliva were also added exactly following the order in Table 4 to avoid salt precipitation, and then was adjusted to pH 6.5 using a NaOH solution (1 M). For both simulated body fluids, NaN_3 at the level of 100 mg/L was added as the inhibitor for microorganism growth. All biochemical reagents in their highest available grade were purchased from Sigma-Aldrich.

2.3 Sorption and desorption experiments

The sorption and desorption experiments were conducted in dark in amber glass vials (40 mL) equipped with Teflon-

Table 1 Selected physicochemical properties of two target soils

Sample	SSA	Organic fractions			Organic constituents			Mineral constituents			
	m^2/g	FA (g/kg)	HA (g/kg)	Humin (g/kg)	TOC (wt%)	C/N*	H/C*	SiO_2 (wt%)	Al_2O_3 (wt%)	Fe_2O_3 (wt%)	CaO (wt%)
YS	37.56	2.30	7.90	11.47	2.01	15.02	9.11	38.69	23.92	12.14	0.22
LS	12.69	5.17	6.70	14.97	3.12	10.81	4.00	59.10	14.16	6.00	2.16

* Atomic ratio

Table 2 Chemical shift of CPMAS ^{13}C-NMR spectra and relative proportions of different carbon types of the sorbents

Sample	0–45 Alkyl C	45–110 O-alkyl C	60–110 Hydrocarbon C	110–140 Aromatic C	140–160 Phenolic C	160–185 Carboxyl C	185–230 Carbonyl C	A/O-A[a]	Ho/Hi[b]
YS	16.69	7.51	30.19	20.74	11.29	9.18	4.41	0.55	0.95
LS	15.63	7.98	30.84	19.65	10.29	10.28	5.34	0.51	0.84

[a]: A/O-A = alkyl C/O-alkyl C = Area(0–45)/Area(45–110);

[b]: Ho/Hi = hydrophobic C/hydrophilic C = Area[(0–45) + (110–160)]/Area[(45–110) + (160–230)]

Table 3 Composition lists for simulated lung fluid and simulated saliva

Adding order	Lung fluid simulation		Saliva simulation	
	Chemical	Concentration (g/L)	Chemical	Concentration (g/L)
1	Magnesium chloride	0.095	α-amylase	0.145
2	Sodium chloride	6.019	Mucin	0.005
3	Potassium chloride	0.298	Urea	0.200
4	Disodium hydrogen phosphate	0.126	Uric acid	0.015
5	Sodium sulphate	0.063	Potassium chloride	0.895
6	Calcium chloride dihydrate	0.368	Potassium thiocyanate	0.200
7	Sodium acetate	0.574	Sodium sulphate	0.570
8	Sodium hydrogen carbonate	2.604	Sodium chloride	0.290
9	Sodium citrate dihydrate	0.097	Sodium dihydrogen phosphate	0.885

Table 4 Parameters of fitted Freundlich sorption isotherms

Samples	Phenanthrene			Pyrene		
	n	$\log K_F$ [(μg/kg)/(μg/L)^n]	R^2	*n*	$\log K_F$ [(μg/kg)/(μg/L)^n]	R^2
Yellow soil (YS)						
Groundwater	0.722 ± 0.014	3.118 ± 0.020	0.992	0.724 ± 0.007	3.648 ± 0.006	0.998
Lung fluid	0.805 ± 0.017	2.856 ± 0.026	0.993	0.763 ± 0.008	3.355 ± 0.006	0.998
Saliva	0.836 ± 0.008	2.845 ± 0.012	0.998	0.865 ± 0.015	3.344 ± 0.011	0.994
Lime soil (LS)						
Groundwater	0.672 ± 0.014	3.323 ± 0.019	0.991	0.663 ± 0.008	3.846 ± 0.007	0.997
Lung fluid	0.718 ± 0.010	3.021 ± 0.016	0.997	0.590 ± 0.018	3.587 ± 0.016	0.982
Saliva	0.622 ± 0.018	3.327 ± 0.025	0.984	0.630 ± 0.014	3.779 ± 0.012	0.991

lined caps (Fisher Scientific) on a temperature-controlled shaker (SY-550B, Taisite Instrument, China) with a rotation speed of 120 rpm. The sorbates, phenanthrene and pyrene, were introduced into the glass vials by spiking predetermined volumes of stock solutions to achieve a series of initial concentrations. The original stock solutions of phenanthrene (1000 ppm) and pyrene (150 ppm) were prepared by dissolving determined amount of each chemical in a 100 mL glass flask with methanol (HPLC grade), and then original stock solutions were diluted sequentially with methanol to make stock solutions of desired concentrations. The operation procedures of the sorption and desorption experiment with simulated groundwater, simulated lung fluid or simulated saliva were identical except the applied solutions.

Briefly, the sorption experiment was conducted triplicate in batch reactors using amber glass vials (40 mL) with Teflon-lined caps, a certain amount of sorbent was carefully weighted into the amber glass vial, filled with the blank solution, a predetermined volume of stock solution was spiked, and then additional blank solution was added to minimize the head space of the vial (less than 0.1 mL). The vial was set horizontally in the temperature-controlled shaker for shaking at 120 rpm at a temperature of 37 °C. Preliminary tests had showed that 14 d was sufficient to attain of the apparent sorption equilibrium for tested soils, therefore, the duration of sorption and desorption experiments was set as 14 d. After shaking, the vial was set upright stilly for 3 d in dark to settle the suspended sorbent completely. An aliquot of the supernatant was taken from the vial into a prepared 5 mL glass vial with pre-weighted methanol (about 2 mL) for stabilization of phenanthrene and pyrene in the vial, the 5 mL glass vial was then stored at 4 °C in the dark waiting for later measurements. The desorption experiment was conducted immediately after the sorption experiment. Briefly, the supernatant left in the vial was carefully removed as much as possible by siphon, then the corresponding blank solution was filled to minimize the headspace of the vial, the vial was capped, set horizontally in the shaker, and operated the rest steps identically as in the sorption experiment. A control experiment of no sorbent in the vial was conducted accompanying to quantify the loss of solute during experiments and was used as a reference in the data reduction.

2.4 Instrumental analysis and calculations

The initial solution concentrations of phenanthrene and pyrene at the start of the experiment and their equilibrium solution concentrations in supernatants obtained after sorption and desorption experiments were determined by an ultra-high-performance-liquid-chromatography (UPLC, Agilent 1290) equipped with diode array UV detector (G4212A), fluorescence detector (G1321B) and auto-sampler unit (G4226A), using an Eclipse XDB-C18 column (2.1 × 150 mm, 3.5 μm) at the column temperature of 37 °C. The sorbate concentration in the supernatant or initial solution was calculated by manipulating the UPLC measured sorbate concentration with a corresponding dilution factor based on the mass ratio of methanol and water in the mixture.

The sorbent-phase sorbate concentrations were computed based on the mass balance of sorbate in the vial with the following equation:

$$q_e = \frac{(C_0 - C_e)V}{M} \tag{1}$$

where q_e is the equilibrium concentration of sorbate in sorbent (μg/Kg); C_0 *and* C_e are initial and equilibrium concentrations of sorbate in solution (μg/L), respectively; V and M are solution volume (L) and sorbent mass (kg) introduced to the vial, respectively.

3 Results and discussion

The Freundlich isotherm model was commonly applied to describe behaviors of HOC sorption/desorption on soil and sediment. It has the following form:

$$q_e = K_F \cdot C_e^n \tag{2}$$

however, the initial sorbate concentrations in the experiment were designed to distribute evenly at the logarithmic scale, therefore, the logarithmic format Freundlich equation (Eq. 3) was applied to achieve a better data fitting

$$\log q_e = \log K_F + n \cdot C_e \tag{3}$$

where K_F is the sorption capacity-related parameter [(μg/kg)/(μg/L)$^\mathrm{n}$] and n is the index of the isotherm linearity.

The organic carbon content normalized single-point distribution coefficient (K_OC) was also often applied to evaluate the distribution level of sorbate between solution and sorbent and can be calculated by Eq. 4:

$$K_D = \frac{q_e}{C_e \times f_{OC}} \tag{4}$$

where q_e is the calculated sorbate concentration in sorbent at a selected C_e by the fitted Freundlich equation, f_oc is the total organic carbon content of the sorbent.

3.1 Sorption experiments

3.1.1 Isotherm nonlinearity

The data presented in Table 4 and Fig. 1 indicated that all measured sorption isotherms are nonlinear, n values ranged

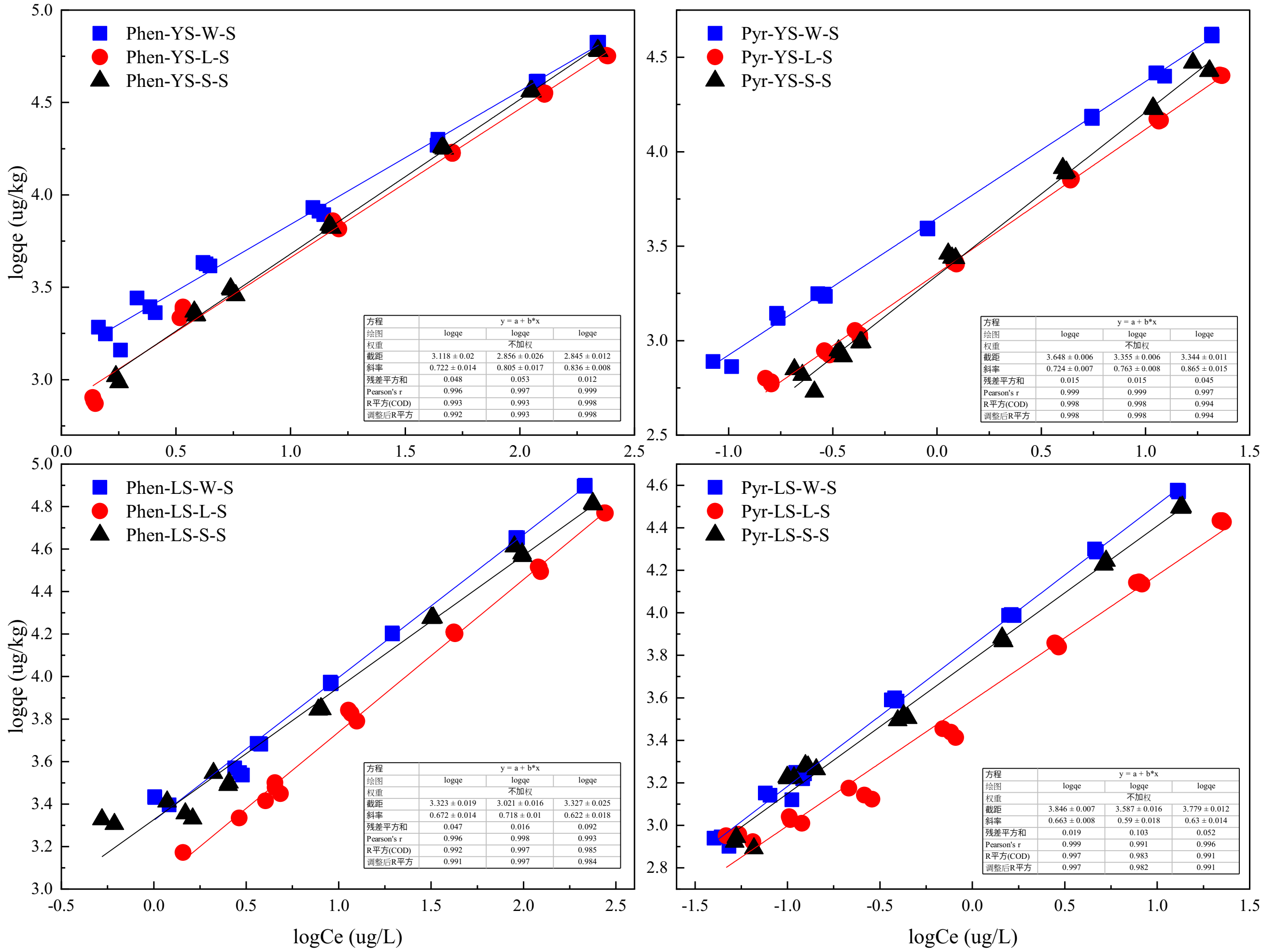

方程	y = a + b*x		
绘图	logqe	logqe	logqe
权重	不加权		
截距	3.118 ± 0.02	2.856 ± 0.026	2.845 ± 0.012
斜率	0.722 ± 0.014	0.805 ± 0.017	0.836 ± 0.008
残差平方和	0.048	0.053	0.012
Pearson's r	0.996	0.997	0.999
R平方(COD)	0.993	0.993	0.998
调整后R平方	0.992	0.993	0.998

方程	y = a + b*x		
绘图	logqe	logqe	logqe
权重	不加权		
截距	3.648 ± 0.006	3.355 ± 0.006	3.344 ± 0.011
斜率	0.724 ± 0.007	0.763 ± 0.008	0.865 ± 0.015
残差平方和	0.015	0.015	0.045
Pearson's r	0.999	0.999	0.997
R平方(COD)	0.998	0.998	0.994
调整后R平方	0.998	0.998	0.994

方程	y = a + b*x		
绘图	logqe	logqe	logqe
权重	不加权		
截距	3.323 ± 0.019	3.021 ± 0.016	3.327 ± 0.025
斜率	0.672 ± 0.014	0.718 ± 0.01	0.622 ± 0.018
残差平方和	0.047	0.016	0.092
Pearson's r	0.996	0.998	0.993
R平方(COD)	0.992	0.997	0.985
调整后R平方	0.991	0.997	0.984

方程	y = a + b*x		
绘图	logqe	logqe	logqe
权重	不加权		
截距	3.846 ± 0.007	3.587 ± 0.016	3.779 ± 0.012
斜率	0.663 ± 0.008	0.59 ± 0.018	0.63 ± 0.014
残差平方和	0.019	0.103	0.052
Pearson's r	0.999	0.991	0.996
R平方(COD)	0.997	0.983	0.991
调整后R平方	0.997	0.982	0.991

Fig. 1 Sorption isotherms of phenanthrene and pyrene on two soils in three different solutions and their Freundlich model fitting results. Note: Phen-YS-W-S and Pyr-YS-W-S: soprion isotherms of phenanthrene and pyrene on yellow soil in the simulated groundwater, repsectively; Phen-YS-L-S and Pyr-YS-L-S: sorption isotherms of phenanthrene and pyrene on yellow soil in the simulated lung fluid, respectively; Phen-YS-S–S and Pyr-YS-S–S: sorption isotherms of phenanthrene and pyrene on yellow soil in the simulated saliva, respectively; Phen-LS-W-S and Pyr-LS-W-S: soprion isotherms of phenanthrene and pyrene on limestone soil in the simulated groundwater, respectively; Phen-LS-L-S and Pyr-LS-L-S: soprion isotherms of phenanthrene and pyrene on limestone soil in the simulated lung fluid, respectively; Phen-LS-S–S and Pyr-LS-S–S: soprion isotherms of phenanthrene and pyrene on limestone soil in the simulated saliva, respectively

from 0.622 to 0.836 for phenanthrene and from 0.590 to 0.865 for pyrene. For phenanthrene sorption, the lowest *n* value, 0.622, showed in the scenario of limestone soil and simulated saliva while the highest, 0.836, in the yellow soil in simulated saliva scenario; for pyrene sorption, the lowest *n* value, 0.590, happened in the limestone soil and simulated lung fluid scenario and the highest, 0.865, showed in the yellow soil in simulated saliva scenario. The different nonlinearities of sorption isotherms of two sorbates on two soils in three different solutions could be the integration results from different properties of sorbates, sorbents, and solutions. It was suggested that SOM is the dominant fraction of soil to uptake or store HOCs (Chiou et al. 1979) while the overall sorption behavior is mainly attributed to SOM compositions, like soft carbon and hard carbon. Linear sorption isotherm for organic matter often results from absorption or partitioning into amorphous organic carbon, which is called "soft carbon", such as fulvic acid and humic acid, while nonlinear sorption isotherm is usually related to a slow process of adsorption or diffusion into heterogeneous sorption sites on condensed organic carbon which is called "hard carbon", such as humin (Carmo et al. 2000; Xiao et al. 2004; Duan and Naidu 2013). In general, no matter phenanthrene or pyrene, sorption nonlinearities of the limestone soil were obviously higher than corresponding those of the yellow soil (Table 4), which is consistent with different SOM compositions of the limestone soil and the yellow soil, the limestone soil had a higher content of humin (14.97 wt%) while the yellow soil had the lower (11.47 wt%, Table 1). Nevertheless, the complexity of soil aggregation structure and chemical figures of SOM may make it particularly challenging to predict the overall sorption behavior for soils based on quantitative analyses of different SOM fractions and their respective sorption equilibria (Huang et al. 2003; Xiao et al. 2004). The sorption nonlinearities of phenanthrene and pyrene on the yellow soil in simulated body fluids are significantly lower than corresponding those in the simulated groundwater (Table 4), which may be attributed to the sorption site competition of organic compounds in body fluids and phenanthrene/pyrene, however, sorption of phenanthrene/pyrene on the limestone soil didn't give expression to this phenomenon, which may be resulted from the much higher content of calcium ion in the limestone soil and the relative higher content of "soft carbon" fractions, fulvic acid and humic acid, since the high content of calcium ion may significantly modify physical conformations of fulvic acid and humic acid and such cast shadow on their sorption behaviors (Simpson et al. 2003; Gao et al. 2006; Chien et al. 2010).

3.1.2 Sorption capacities

It is suggested that $\log K_F$, the fitted parameter of the Freundlich model is related closely to the sorption capacity (Gunasekara and Xing 2003). As shown in Table 4, $\log K_F$ values varied from 2.845 to 3.327 for phenanthrene and from 3.344 to 3.779 for pyrene, consistent with the fact that the more hydrophobic pyrene inclines to stay with soil in the aqueous environment more than phenanthrene does. Different geosorbents exhibited different sorption capacities due to their different natures. The limestone soil showed much more sorption capacity, $\log K_F$ ranged from 3.021 to 3.327, compared to that of the yellow soil, $\log K_F$ ranged from 2.845 to 3.118, which, however, is contradicted to their specific surface area (SSA) data measured by N_2-BET (Table 1), the SSA of the limestone soil is 12.69 m^2/g and smaller than that of the yellow soil (37.56 m^2/g). The higher sorption capacities of the limestone soil must be attributed to its higher TOC content (3.12 wt%). The calculated organic carbon normalized single point distribution coefficient (K_{OC}) values, on the other hand, indicated that the SOM of the yellow soil has higher sorption capacities of both phenanthrene and pyrene in all circumstances except the simulated saliva (Table 5), which is agreed with the higher A/O-A and Ho/Hi ratios of SOM in the yellow soil (Table 2). The A/O-A and Ho/Hi ratios are suggested as the proxies of SOM's hydrophobicity (Chung et al. 2012), the higher hydrophobicity is, the better the quality of SOM is for sorption HOCs (Huang et al. 2003). Interactions among simulated saliva compounds and SOM fractions of the limestone soil may enhance the sorption of phenanthrene/pyrene, especially at their low equilibrium concentration end, where their $\log K_F$ and K_{OC} values are very closed to those for the simulated groundwater and significantly higher than those for the simulated lung fluid. Nevertheless, the underlying mechanism is largely uncertain. It can be seen easily from Fig. 1, sorption capacities varied in different solution systems, highest in the simulated groundwater and lowest in the simulated lung fluid, as showed in Fig. 1, the isotherms measured in the simulated lung fluid (red dots) locate below other isotherms and the isotherms measured in the simulated groundwater (blue square) locate above other isotherms.

3.2 Desorption experiments

3.2.1 Desorption isotherm

The desorption experiments were conducted immediately after the equilibrium sorption experiments under the same experimental conditions. All desorption isotherms were plotted in Fig. 2. The n values for desorption isotherms were generally lower and the $\log K_F$ values for desorption isotherms were significantly higher than corresponding those of sorption isotherms (Tables 4 and 6), indicating that the resistant fraction of phenanthrene/pyrene tended to stay on "high energy sites" and the desorption is not a reverse process of the sorption. The variation trends of Freundlich parameters for sorption and desorption were complex, they varied for two different sorbents, the yellow soil and the limestone soil, two different sorbates, phenanthrene and pyrene, as well as the three different solutions, simulated groundwater, lung fluid, and saliva. Briefly, for the n value of phenanthrene desorption isotherm in the simulated groundwater, it was 0.662 for the yellow soil, decreased by 0.06 from that of the sorption isotherm (0.722), but was 0.744 for the limestone, increased by 0.072, from that of the sorption isotherm (0.672), the different variation trends may be resulted from the change of the soil conformation under a relatively high temperature of 37 °C during 4 weeks experiment time and/or from the loss of soluble SOM in the supernatant removal at the beginning of the desorption experiment. But the universality of this phenomenon is waiting for more studies. No consistent variation trends were observed for other desorption experiments either, likely indicating the effects of soil conformation changes and the loss of soluble SOM between sorption and desorption experiments. The $\log K_F$ values for desorption isotherms increased significantly from corresponding to those of sorption isotherms, suggesting the existence of irreversible sorption. The K_{OC} values calculated for desorption experiments (Table 7)

Table 5 Calculated K_{oc} values for sorption experiments ($\times 10^4$ L/kg)

Samples	Solution	Phenanthrene C_e (μg/L)			Pyrene C_e (μg/L)		
		3	30	300	0.3	3	30
YS	Groundwater	4.810	2.536	1.337	16.335	8.652	4.583
	Lung fluid	2.882	1.840	1.174	8.684	5.032	2.916
	Saliva	2.908	1.993	1.366	10.571	9.752	8.997
LS	Groundwater	4.703	2.210	1.038	15.526	7.146	3.289
	Lung fluid	2.468	1.289	0.673	7.893	3.071	1.195
	Saliva	4.493	1.881	0.788	12.832	5.474	2.335

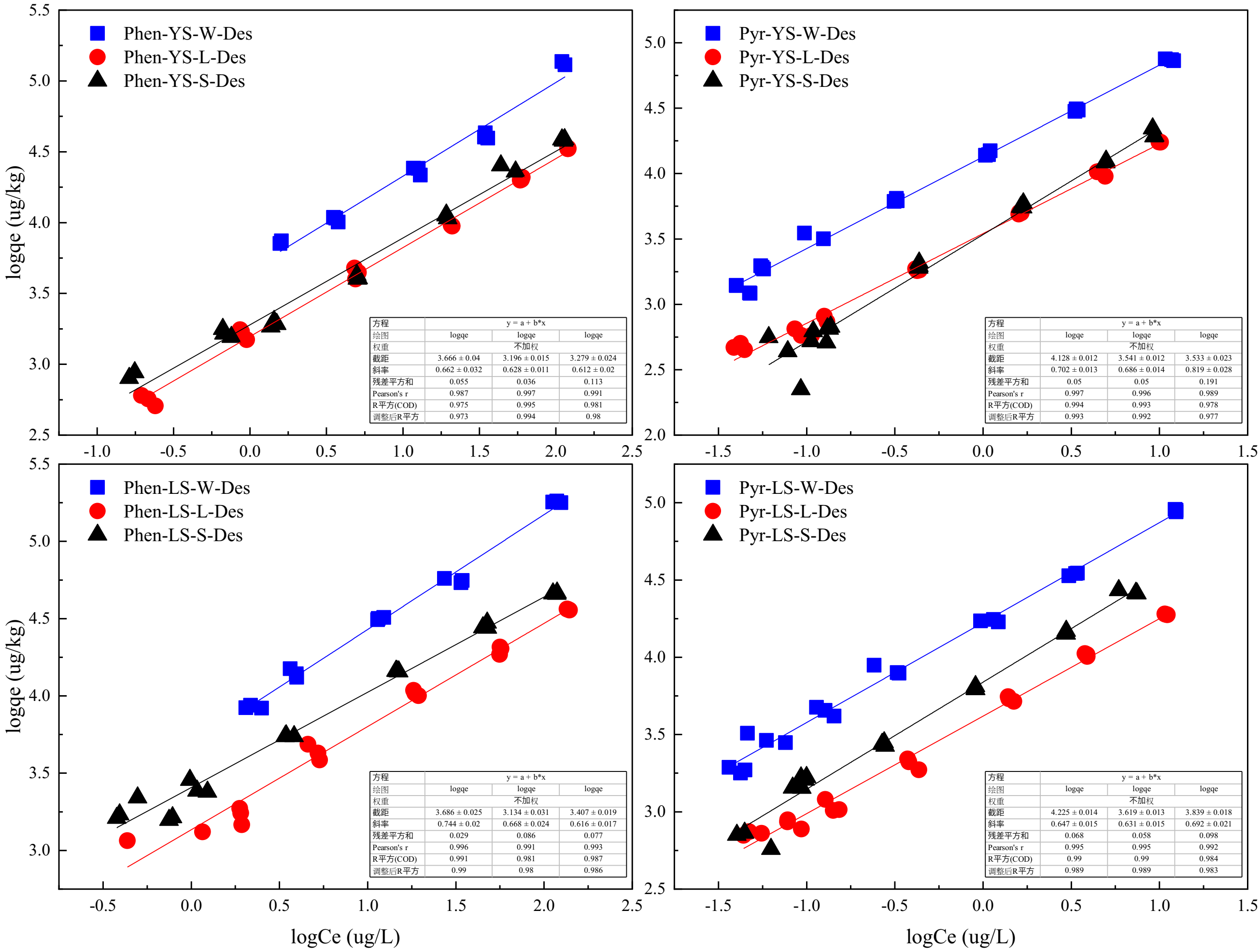

方程	y = a + b*x		
绘图	logqe	logqe	logqe
权重	不加权		
截距	3.666 ± 0.04	3.196 ± 0.015	3.279 ± 0.024
斜率	0.662 ± 0.032	0.628 ± 0.011	0.612 ± 0.02
残差平方和	0.055	0.036	0.113
Pearson's r	0.987	0.997	0.991
R平方(COD)	0.975	0.995	0.981
调整后R平方	0.973	0.994	0.98

方程	y = a + b*x		
绘图	logqe	logqe	logqe
权重	不加权		
截距	4.128 ± 0.012	3.541 ± 0.012	3.533 ± 0.023
斜率	0.702 ± 0.013	0.686 ± 0.014	0.819 ± 0.028
残差平方和	0.05	0.05	0.191
Pearson's r	0.997	0.996	0.989
R平方(COD)	0.994	0.993	0.978
调整后R平方	0.993	0.992	0.977

方程	y = a + b*x		
绘图	logqe	logqe	logqe
权重	不加权		
截距	3.686 ± 0.025	3.134 ± 0.031	3.407 ± 0.019
斜率	0.744 ± 0.02	0.668 ± 0.024	0.616 ± 0.017
残差平方和	0.029	0.086	0.077
Pearson's r	0.996	0.991	0.993
R平方(COD)	0.991	0.981	0.987
调整后R平方	0.99	0.98	0.986

方程	y = a + b*x		
绘图	logqe	logqe	logqe
权重	不加权		
截距	4.225 ± 0.014	3.619 ± 0.013	3.839 ± 0.018
斜率	0.647 ± 0.015	0.631 ± 0.015	0.692 ± 0.021
残差平方和	0.068	0.058	0.098
Pearson's r	0.995	0.995	0.992
R平方(COD)	0.99	0.99	0.984
调整后R平方	0.989	0.989	0.983

Fig. 2 Desorption isotherms of phenanthrene and pyrene on two soils in three different solutions and their Freundlich model fitting results. Note: Phen-YS-W-Des and Pyr-YS-W-Des: desorption isotherms of phenanthrene and pyrene on yellow soil in the simulated groundwater, repsectively; Phen-YS-L-Des and Pyr-YS-L-Des: desorption isotherms of phenanthrene and pyrene on yellow soil in the simulated lung fluid, respectively; Phen-YS-S-Des and Pyr-YS-S-Des: desorption isotherms of phenanthrene and pyrene on yellow soil in the simulated saliva, respectively; Phen-LS-W-Des and Pyr-LS-W-Des: desorption isotherms of phenanthrene and pyrene on limestone soil in the simulated groundwater, respectively; Phen-LS-L-Des and Pyr-LS-L-Des: desorption isotherms of phenanthrene and pyrene on limestone soil in the simulated lung fluid, respectively; Phen-LS-S-Des and Pyr-LS-S-Des: desorption isotherms of phenanthrene and pyrene on limestone soil in the simulated saliva, respectively

Table 6 Parameters of fitted Freundlich desorption isotherms

Samples	Phenanthrene			Pyrene		
	n	logK_F [(μg/kg)/(μg/L)^n]	R^2	*n*	logK_F [(μg/kg)/(μg/L)^n]	R^2
Yellow soil (YS)						
Groundwater	0.662 ± 0.032	3.666 ± 0.040	0.973	0.702 ± 0.013	4.128 ± 0.012	0.993
Lung fluid	0.628 ± 0.011	3.196 ± 0.015	0.994	0.686 ± 0.014	3.541 ± 0.012	0.992
Saliva	0.612 ± 0.020	3.279 ± 0.024	0.980	0.819 ± 0.028	3.533 ± 0.023	0.977
Lime soil (LS)						
Groundwater	0.744 ± 0.020	3.686 ± 0.025	0.990	0.647 ± 0.015	4.225 ± 0.014	0.989
Lung fluid	0.668 ± 0.024	3.134 ± 0.031	0.980	0.631 ± 0.015	3.619 ± 0.013	0.989
Saliva	0.616 ± 0.017	3.407 ± 0.019	0.986	0.692 ± 0.021	3.839 ± 0.018	0.983

Table 7 Calculated K_{oc} values for desorption experiments (× 10^4 L/kg)

Samples	Solution	Phenanthrene C_e (μg/L)			Pyrene C_e (μg/L)		
		3	30	300	0.3	3	30
YS	Groundwater	15.905	7.304	3.354	48.153	24.245	12.207
	Lung fluid	5.192	2.205	0.936	12.246	5.943	2.884
	Saliva	6.176	2.527	1.034	13.914	9.172	6.046
LS	Groundwater	11.741	6.512	3.612	36.511	16.197	7.185
	Lung fluid	3.030	1.411	0.657	8.888	3.800	1.625
	Saliva	5.366	2.216	0.915	15.772	7.761	3.818

were also greater than corresponding those for sorption experiments (Table 5). Both logK_F and K_{OC} values demonstrated, compared to the simulated groundwater, simulated body fluids, especially the simulated lung fluid, were not favorable for HOCs sorption on the target soils.

3.2.2 *Sorption–desorption hysteresis*

Almost all samples performed that the *n* values of desorption isotherms were lower than corresponding those of sorption isotherms, while the capacities of desorption were higher than corresponding those of sorption, suggesting the non-ideal irreversible processes of sorption and desorption which can be evaluated by the Hysteresis Index (*HI*) defined by Eq. (5):

$$Hysteresis\ Index = \frac{q_e^d - q_e^s}{q_e^s} \tag{5}$$

where q_e^s and q_s^d are solid-phase sorbate concentrations for a single-cycle sorption and desorption experiment, respectively. The *HI* values of phenanthrene and pyrene sorption–desorption in three solutions at three different peer concentration levels were calculated and list in Table 8. All the samples performed the desorption hysteresis phenomenon at the three solute concentrations levels. It is suggested that the entrapment of sorbate molecules within condensed SOM matrices plays an important role in sorption–desorption hysteresis (Pignatello 1998; Huang et al. 2003). The decreasing of *HI* values with increasing of the concentration level is due to the

Table 8 Calculated *HI* values for phenanthrene and pyrene on two soils in three different solution systems

Samples	Solution	Phenanthrene C_e (μg/L)			Pyrene C_e (μg/L)		
		3	30	300	0.3	3	30
YS	Groundwater	2.307	1.880	1.508	1.948	1.802	1.664
	Lung fluid	0.801	0.198	-0.203	0.410	0.181	-0.011
	Saliva	1.124	0.268	-0.243	0.316	-0.060	-0.328
LS	Groundwater	1.497	1.947	2.478	1.352	1.267	1.185
	Lung fluid	0.228	0.094	-0.025	0.126	0.238	0.360
	Saliva	0.194	0.178	0.162	0.229	0.418	0.635

occupation priority of high energy sites, less proportion HOCs molecules sorbed on high sorption energy site can be released in desorption and such cause the higher HI value. The prior studies had shown that hysteretic sorption appears to be associated with the reduced and condensed SOM domain matrices (Xing et al., 1996; Huang et al. 2003), which was verified in experiments in the simulated groundwater of this study. The yellow soil showed higher

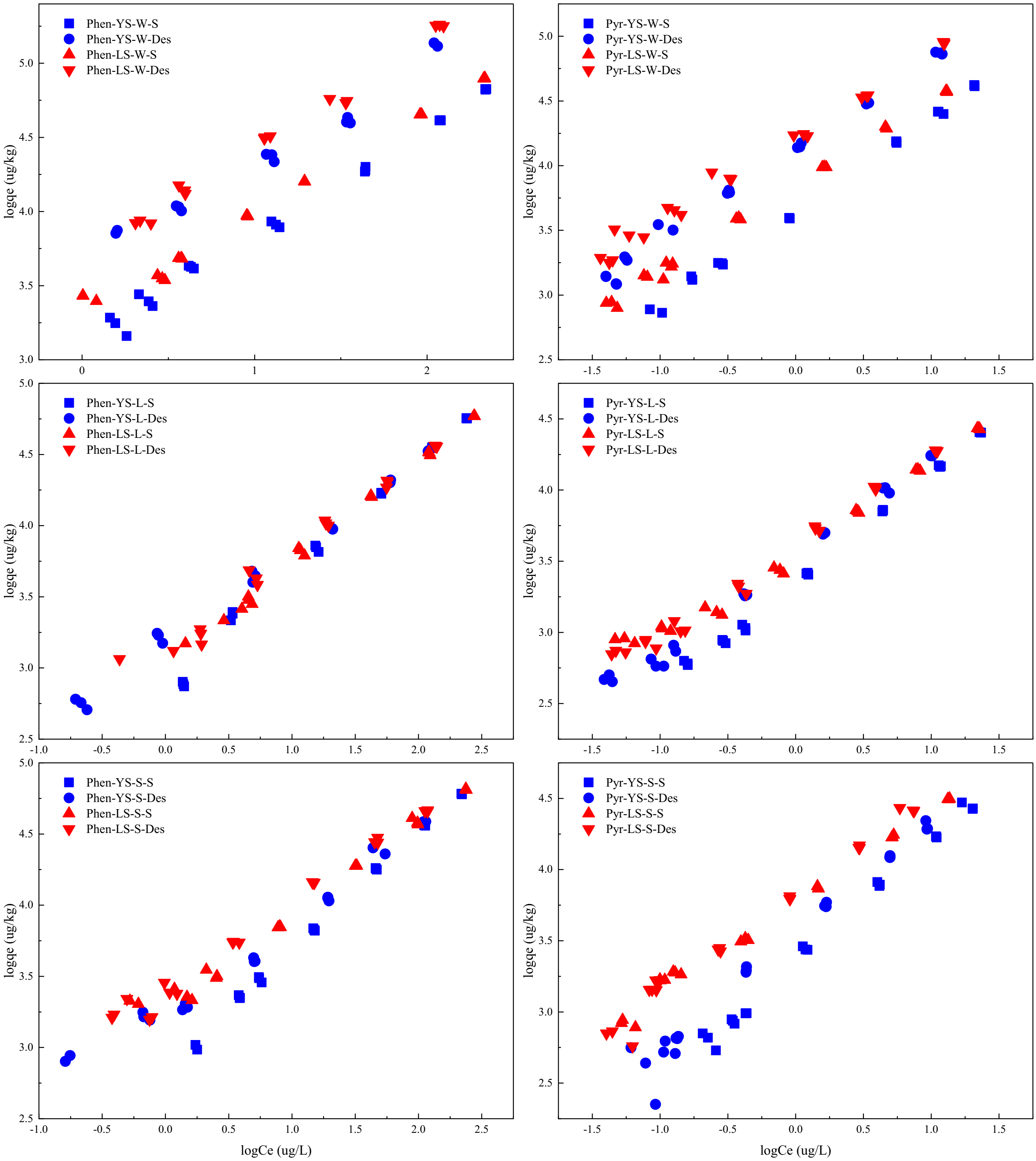

Fig. 3 Comparison of sorption–desorption behaviors of phenanthrene and pyrene on two soils in three different solutions. Note: Legends are the same as those in Figs. 1 and 2

HI values likely because its SOM is more hydrophobic and its condensed carbon proportion is higher. But this trend was not manifested in experiments in simulated body fluids, by and large, the *HI* values for the simulated body fluids experiment systems were small, a couple of sorption–desorption isotherms were even overlapped (Fig. 3), probably due to complex interactions among large organic chemicals of simulated body fluids, sorbate molecules, and functional groups at surfaces of SOM.

4 Discussion

Due to the high hydrophobicity of PAHs, once released into the natural environment, PAHs tend to accumulate in soil and sediment and bind primarily with SOM, and their aqueous concentrations are exceptionally low (Wilcke 2000; Ni et al. 2008; Yang et al. 2014; Yu et al. 2014). The contaminated soil and sediment acts as the secondary sources of PAHs and casts durative risks to the surrounding environment (Cornelissen et al. 1997; Shor et al. 2003). Therefore, the comprehensive understanding of sorption–desorption behaviors of PAHs on typical soils in a region is of significance to precisely assessing the fate and environmental risks of PAHs in this region. Yellow soil and limestone soil are the two most occurring natural soils of the southwest China karst area, taking up 65% of the surface soil area of Guizhou Province. However, practical data regarding how their natures that affect the sorption and desorption of PAHs are scarce. In this study, we reported the sorption–desorption isotherms and fitted Freundlich parameters for the yellow soil and the limestone soil. The results indicated that, although the TOC contents of the yellow soil and the limestone soil (2.01% and 3.12%, respectively) are remarkable lower than that of the Chelsea soil (5.45%) (Huang, 1997), a surface soil frequently used in prior sorption studies, their phenanthrene sorption and desorption capacity parameters ($\log K_F$), 3.118 and 3.648 for the yellow soil and 3.323 and 3.846 for the limestone, are comparable to those of the Chelsea soil (3.644 and 3.658), accordingly their K_{OC} values are even higher. The possible explanation can attribute to the characteristics of the two soils, they contained relatively high contents of humin (“hard carbon”), which is consistent with that both two soils were developed from the weathering residuals of carbonate rocks, which may contain old and deeply metamorphic organic matters. The relatively large *HI* values of the two soils (Table 8) further manifested that PAHs pollutants may undergo natural sequestration through partially irreversible sorption processes.

The different sorption–desorption behaviors of phenanthrene and pyrene on two soils in the three different solution systems demonstrated the influences of inorganic salts, organic acids, and proteins in the simulated body fluids. Generally, sorption–desorption isotherms of phenanthrene and pyrene in the simulated body fluids were relatively more linear and the sorption capacities were lower compared to those in the simulated groundwater experiments. The hydrophobic region of α-amylase and mucin could interact with hydrophobic phenanthrene and pyrene, leading to lower interaction between hydrophobic organic compounds and soil particles (Wang et al. 2011a, b). With the change of ionic strength, the DOC content in the solution would be different consequently, resulted in a difference of sorption of phenanthrene and pyrene, because a micelle-like structure of DOC would be formed following the addition of cations (Duan and Naidu 2013). However, once the DOC concentration was high, intra- and interactions could block certain sorption sites, lead to a smaller sorption amount because of the change in surface charge density. The constitutions of simulated lung fluid and saliva were different, in addition to different SOM natures of yellow soil and limestone soil, lead to different associated DOC contents and prosperities, and resulted in different sorption behaviors in consequence. Although the underlying mechanisms of the different sorption–desorption behaviors of PAHs on two soils in the simulated body fluids and in the simulated groundwater were complicated and demand more studies, the lower sorption capacity and small sorption–desorption hysteresis suggested that direct application of sorption–desorption experiment data from the simulated groundwater system may cause erroneous estimations of bioavailability and health risk of PAHs retained in soils.

5 Conclusions

In summary, this study selected phenanthrene and pyrene as the representative PAHs and investigated their sorption–desorption behaviors on two major soils in the southwest China karst area. Sorption–desorption onto these two types of soils in three different solutions, simulated groundwater, simulated lung fluid, and simulated saliva, were studied. The experimental results showed that the yellow soil and limestone soil have a relatively high ability to retentate PAHs and therefore can serve as a pool of PAHs pollutants in the study region. The sorbent nature and sorbate hydrophobicity dominated the sorption and desorption behaviors of the two PAHs. All measured sorption–desorption isotherms fit well with the Freundlich model. The experimental results further indicated that sorption and desorption behaviors of PAHs in the simulated groundwater were quite different from those in the simulated body fluids. The sorption capacities and the sorption nonlinearities of PAHs on the soils were significantly lower in simulated body fluids than in simulated groundwater, which suggested that the bioavailability and the health risk of PAHs in contaminated soils may be underestimated if the data from simulated sorption–desorption experiments in groundwater were directly applied.

Acknowledgements This research was supported by the National Natural Science Foundation of China-Guizhou Joint Fund for Karst Science Research Center (U1612441), National Natural Science Foundation of China (41173129, 41273149), and the S&T Plan Project of Guizhou (2011-3109).

Compliance with Ethical Standards

Conflict of interest On behalf of all authors, the corresponding author states that there is no conflict of interest.

References

Abelmann K, Kleineidam S, Knicker H, Grathwohl P, Kögel-Knabner I (2005) Sorption of HOC in soils with carbonaceous contamination: influence of organic-matter composition. J Plant Nutr Soil Sci 168:293–306

Ball W, Roberts P (1991) Long-term sorption of halogenated organic chemicals by aquifer material. 2. Intraparticle diffusion Environ Sci Technol 25:1223–1237

Barnier C, Ouvrard S, Robin C, Morel J (2014) Desorption kinetics of PAHs from aged industrial soils for availability assessment. Sci Total Environ 470–471:639–645

Bonin JL, Simpson MJ (2007) Variation in phenanthrene sorption coefficients with soil organic matter fractionation: the result of structure or conformation? Environ Sci Technol 41:153–159

Brusseau M, Rao P, Gillham R (1989) Sorption nonideality during organic contaminant transport in porous media. Crit Rev Environ Control 19:33–99

Carmicheal L, Christman R, Pfaener F (1997) Desorption and mineralization kinetics of phenanthrene and chrysene in contaminated soils. Environ Sci Technol 31:126–132

Carmo A, Hundal L, Thompson M (2000) Sorption of hydrophobic organic compounds by soil materials: application of unit equivalent Freundlich coefficients. Environ Sci Technol 34:4363–4369

Chien CSW, Chen CY, Chang JH, Chen SH, Wang MC, Mannepalli MR (2010) Sorption of toluene by humic acids derived from lake sediment and mountain soil at different pH. J Hazard Mater 177:1068–1076

Chin Y, Aiken G, Danielsen K (1997) Binding of Pyrene to aquatic and commercial humic substances: the role of molecular weight and aromaticity. Environ Sci Technol 31:1630–1635

Chiou C, Peters L, Freed V (1979) A physical concept of soil-water equilibrium for non-ionic organic compounds. Science 206:831–832

Chung TL, Chen JS, Chiu CY, Tian GL (2012) ^{13}C-NMR spectroscopy studies of humic substances in subtropical perhumid montane forest soil. J For Res 17(6):458–467

Colombo C, Monhemius AJ, Plant J (2008) Platinum, palladium and rhodium release from vehicle exhaust catalysts and road dust exposed to simulated lung fluids. Ecotoxicol Environ Saf 71:722–730

Cornelissen G, Gustafsson O (2005) Importance of unburned coal carbon, black carbon, and amorphous organic carbon to phenanthrene sorption in sediments. Environ Sci Technol 39:764–769

Cornelissen G, van Noort P, Govers H (1997) Desorption kinetics of chlorobenzenes, polycyclic aromatic hydrocarbons, and polychlorinated biphenyls: sediment extraction with Tenax and effects of contanct time and solute hydrophobicity. Environ Toxicol Chem 16:1351–1357

Dean J, Ma R (2007) Approaches to assess the oral bioaccessibility of persistent organic pollutants: A critical review. Chemosphere 68:1399–1407

Di X, Xiao B, Dong H, Wang S (2018) Implication of different humic acid fractions in soils under karst rocky desertification. Catena 174:308–315

Ding G, Novak J, Herbert S, Xing B (2002) Long-term tillage effects on soil metolachlor sorption and desorption behavior. Chemosphere 48:897–904

Duan L, Naidu R (2013) Effect of ionic strength and index cation on the sorption of phenanthrene. Water Air Soil Pollut 224:1700–1717

Farrell J, Hauck B, Jones M (1999) Thermodynamic investigation of trichloroethylene adsorption in water-saturated microporous adsorbents. Environ Toxicol Chem 18:1637–1642

Gao Y, Xiong W, Ling W, Xu J (2006) Sorption of phenanthrene by soils contaminated with heavy metals. Chemosphere 65(8):1355–1361

Ghosh U, Talley J, Luthy R (2001) Particle-scale investigation of PAHs desorption kinetics and thermodynamics from sediment. Environ Sci Technol 35:3468–3475

Gunasekara A, Xing B (2003) Sorption and desorption of naphthalene by soil organic matter: importance of aromatic and aliphatic components. J Environ Qual 32:240–246

Huang W (1995) Sorption and desorption by soils and sediments: effects of sorbent heterogeneity. the University of Michigan, Ann Arbor, MI

Huang W, Weber J (1997) A distributed reactivity model for sorption by soils and sediments. 10. Relationships between desorption, hysteresis, and the chemical characteristics of organic domains. Environ Sci Technol 31:2562–2569

Huang W, Weber J (1998) A distributed reactivity model for sorption by soils and sediments. 11: Slow concentration-dependent sorption rates. Environ Sci Technol 32:3549–3555

Huang W, Yu H, Weber J (1998) Hysteresis in the sorption and desorption of hydrophobic organic contaminants by soils and sediments: 1. a comparative analysis of experimental protocols. J Contam Hydol 31:129–148

Huang W, Peng P, Yu Z, Fu J (2003) Effects of organic matter heterogeneity on sorption and desorption of organic contaminants by soils and sediments. Appl Geochem 18:955–972

Kan A, Fu G, Tomson M (1994) Adsorption/desorption hysteresis in organic pollutant and soil/sediment interaction. Environ Sci Technol 28:859–867

Kan A, Fu G, Hunter M, Chen W, Ward C, Tomson M (1998) Irreversible sorption of neutral hydrocarbons to sediments: experimental observations and model predictions. Environ Sci Technol 32:892–902

LeBoeuf E, Weber J (1997) A distributed reactivity model for sorption by soils and sediments: 8. Identification of a humic acid glass transition and a logic for invoking polymer sorption theory. Environ Sci Technol 3:1697–1702

LeBoeuf E, Weber J (2000a) Macromolecular characteristics of natural organic matter: 1. Insights from glass transitions and enthalpy relaxations. Environ Sci Technol 34:3623–3631

LeBoeuf E, Weber J (2000b) Macromolecular characteristics of natural organic matter: 2. Sorption and desorption behavior. Environ Sci Technol 34:3632–3640

Luo L, Lin S, Huang H, Zhang S (2012) Relationships between aging of PAHs and soil properties. Environ Pollut 170:177–182

Ni J, Luo Y, Wei R, Li X (2008) Distribution patterns of polycyclic aromatic hydrocarbons among different organic carbon fractions of polluted agricultural soils. Geoderma 146:277–282

Pan B, Xing B, Tao S, Liu W, Lin X, Xiao Y, Dai H, Zhang X, Zhang Y, Yuan H (2007) Effect of physical forms of soil organic matter on phenanthrene sorption. Chemosphere 68:1262–1269

Perminova I, Grechishcheva N, Peterosyan V (1999) Relationships between structure and binding affinity of humic substances for polycyclic aromatic hydrocarbons: relevance of molecular descriptors. Environ Sci Technol 33:3781–3787

Pignatello J (1990) Slowly reversible sorption of aliphatic halocarbons in soils. I. Formation of residual fractions. Environ Toxi Chem 9:1107–1115

Pignatello J (1998) Soil organic matter as a nanoporous sorbent of organic pollutants. Adv Coll Interface Sci 76:445–467

Shor LM, Rockne KJ, Taghon GL, Young LY, Kosson DS (2003) Desorption kinetics for field-aged polycyclic aromatic hydrocarbons from sediments. Environ Sci Technol 37:1535–1544

Simpson MJ, Chefetz B, Hatcher PG (2003) Phenanthrene sorption to structurally modified humic acids. J Environ Qual 32:1750–1758

Stopford W, Turner J, Cappellini D, Brock T (2003) Bioaccessibility testing of cobalt compounds. J Environ Monit 5:675–680

Wang W, Simnich S, Giri B, Chang Y, Zhang Y, Jia Y, Tao S, Wang R, Wang B, Li W, Cao J, Lu X (2011a) Atmospheric concentration and air-soil gas exchange of polycyclic aromatic hydrocarbon (PAHs) in remote, rural village and urban areas of Beijing-Tianjin region, North China. Sci Total Environ 409:2942–2950

Wang X, Zhao J, Song L, Mashayekhi H, Chefetz B, Xing B (2011b) Adsorption and desorption of phenanthrene on carbon nanotubes in simulated gastrointestinal fluids. Environ Sci Technol 45:6018–6024

Weber W Jr, Huang W (1996) A distributed reactivity model for sorption by soils and sediments. 4. Intraparticle heterogeneity and phase-distribution relationships under nonequilibrium conditions. Environ Sci Technol 30:881–888

Weber J, Huang W, Yu H (1998) Hysteresis in the sorption and desorption of hydrophobic organic contaminants by soils and sediments: 2. Effects of soil organic matter heterogeneity. J Cont Hydrol 31:149–165

Wehrer M, Tosche K (2009) Difference in PAH release processes from tar-oil contaminated soil materials with similar contamination history. Chem Erde 69(2):109–124

Wilcke W (2000) Polycyclic aromatic hydrocarbons (PAHs) in soil, a review. J Plant Nutr Soil Sci 163:229–248

Wu S, Gschwend G (1986) Sorption kinetics of hydrophobic organic compounds to natural sediments and soils. Environ Sci Technol 20:717–725

Xia Z, Duan X, Tao S, Qiu W, Liu D, Wang Y, Wei S, Wang B, Jiang Q, Lu B, Song Y, Hu X (2013) Pollution level, inhalation exposure and lung cancer risk of ambient atmospheric polycyclic aromatic hydrocarbons (PAHs) in Taiyuan, China. Environ Pollut 173:150–156

Xiao B, Yu Z, Huang W, Song J, Peng P (2004) Black carbon and kerogen in soils and sediments. 2. Their roles in equilibrium sorption of less-polar organic pollutants. Environ Sci Technol 38:5842–5852

Xing B (1997) The effect of the quality of soil organic matter on sorption of naphthalene. Chemosphere 35:633–642

Yang W, Duan L, Zhang N, Zhang C, Shipley H, Kan A, Tomson M, Chen W (2008) Resistant desorption of hydrophobic organic contaminants in typical Chinese soil: implications for long–term fate and soil quality standards. Environ Toxicol Chem 27:235–242

Yang X, Garnier P, Wang S, Bergheaud V, Huang X, Qiu R (2014) PAHs sorption and desorption on soil influenced by pine needle litter-derived dissolved organic matter. Pedosphere 24:575–584

Young K, LeBoeuf E (2000) Glass transition behavior of a peat humic acid and a stream fulvic acid. Environ Sci Technol 34:4549–4553

Yu H, Xiao H, Wang D (2014) Effect of soil properties and biosurfactant on the behavior of PAHs in soil-water systems. Environ Syst Res 3:2193–2697